Journal Article

Octenyl-succinylated inulin for the encapsulation and release of hydrophobic compounds

Han, L., Hu, B., Ratcliffe, I., Senan, C., Yang, J. and Williams, P

Octenyl-succinylated inulin for the encapsulation and release of hydrophobic compounds

Lingyu Han[a,b,†], Bing Hu[b,†], Ian Ratcliffe[c], Chandra Senan[c], Jixin Yang[c] and Peter A. Williams[c,*]

[a]Key Lab of Biotechnology and Bioresources Utilization of Ministry of Education, College of Life Science, Dalian Minzu University, Dalian, Liaoning, 116600, China;
[b]Glyn O. Phillips Hydrocolloid Research Centre at HBUT, School of Food and Biological Engineering, Hubei University of Technology, Wuhan 430068, China;
[c] Centre for Water Soluble Polymers, Applied Science, Faculty of Arts, Science and Technology, Wrexham Glyndwr University, Plas Coch, Mold Road, Wrexham, LL11 2AW United Kingdom.

*Corresponding author: Professor Peter A. Williams, Centre for Water Soluble Polymers, Applied Science, Faculty of Arts, Science and Technology, Wrexham Glyndwr University, Plas Coch, Mold Road, Wrexham, LL11 2AW, United Kingdom.
Telephone: +44 1978 293083
Email: williamspa@glyndwr.ac.uk

† These authors contributed equally to this work.

KEYWORDS: Octenyl-succinylated inulin, critical aggregation concentration, encapsulation, beta-carotene

ABSTRACT:

Octenyl-succinylated inulins (OSA-inulin) were synthesized in aqueous solutions using inulin with varying degrees of polymerization (DP). They were characterized using ^{1}H NMR and FTIR and their degrees of substitution were determined. All the samples formed micellar aggregates in aqueous solution above a critical aggregation concentration (CAC) and solubilized beta-carotene. The amount of beta carotene solubilized within the micelles ranged from 12 -25mg/g of OSA-inulin and depended on the inulin molar mass. Dynamic light scattering showed that the aggregates, with and without dissolved beta-carotene, were ~10-15 nm in size and this was confirmed by Transmission Electron Microscopy which also indicated that the micelles had a globular shape. OSA-inulin particles containing encapsulated beta-carotene were produced by freeze-drying. The encapsulated beta-carotene was not released from the freeze-dried particles when introduced into simulated gastric fluid at pH 2.5 but was readily released in simulated small intestinal fluid at pH 7. The results demonstrate the potential application of OSA-inulin in the encapsulation, dissolution and targeted delivery of hydrophobic drug molecules for nutraceutical, pharmaceutical and medical applications.

1. Introduction

Inulin is a fructan and is composed of β (2→1) linked β-D-fructose residues with degrees of polymerization between 2-60 and has a α-D-glucose residue attached at the reducing end (French, 1993). It is finding increased use in food products because of its ability to form gels at high concentrations and also because it is a type of dietary fibre. It is not absorbed in the stomach or small intestine but is degraded by inulinase produced by bacteria present in the colon leading to the formation of short-chain fatty acids which are considered to have significant health benefits.

We have shown in previous publications that alkenyl succinylated inulins will form micellar aggregates in solution (Kokubun, Ratcliffe, and Williams, 2013; Han, Ratcliffe, & Williams, (2015); Kokubun, Ratcliffe, and Williams, 2018). The micellar aggregates develop at the so-called critical aggregation concentration, CAC, which depends on the length of the alkenyl chains and the degree of substitution (DS). The micellar aggregates have been shown to dissolve hydrophobic compounds and hence have potential applications in a range of industrial sectors. Srinarong, *et al*. (2011) used a commercially available hydrophobically modified inulin (Inutec SP1) to encapsulate a range of hydrophobic drugs by freeze-drying. The particles produced were found to be highly porous and spherical and were shown to readily dissolve in water or phosphate buffer solution to solubilize the drugs. These workers demonstrated that Inutec SP1 was far superior to solid dispersions produced using polyvinylpyrrolidone. Muley *et al*. (2016) investigated the ability of Inutec SP1 to encapsulate the anti-cancer drug, paclitaxel, by using 'thin film hydration' and 'solvent evaporation' techniques. They produced paclitaxel-loaded micelles with a mean size of ~250nm which displayed sustained release of the drug and enhanced anti-cancer efficacy.

Recently we demonstrated that octenyl (OSA-) and dodecenyl- (DDSA-) succinylated inulin could be used to encapsulate beta-carotene through the solvent evaporation method (Kokubun, Ratcliffe & Williams, 2018) and that the efficiency was enhanced at higher DS. The purpose of the present study is to initially prepare a series of high DS octenyl succinylated inulin derivatives using inulin samples with varying molar masses and to subsequently investigate their ability to encapsulate and release

beta-carotene, following freeze-drying.

2. Materials and Method

2.1 Materials

Inulin INUTEC® H25P was supplied by Beneo Biobased Chemicals. It has previously been characterized using MALDI-TOF (Matrix Assisted Laser Desorption Ionisation Time of Flight) Mass Spectrometry and was found to consist of molecules with DP between 2 and 8, consistent with data supplied by the suppliers (Evans, 2014). Fibruline® DS2 and Fibruline XL were supplied by Cosucra Chemicals. The DP of DS2 was deemed to be 2-18 (Han, Ratcliffe & Williams, 2017) while the corresponding value for XL was 20-23 (Ronkart *et al*., 2007). The inulin was dried at 70 °C for 24 hours before use. Octenyl succinic anhydride (OSA) was obtained from Tokyo Chemical Industry UK Ltd, Oxford and was used as received. Beta-carotene powder was obtained from Sigma-Aldrich Chemie GmbH. and used as supplied. Cyclohexane was obtained from Fisher Chemicals. Pepsin from porcine gastric mucosa was obtained from Sigma-Aldrich Chemie GmbH. and used as supplied. Bile salt No.3 (69005060) was obtained from Sinopharm Chemical Reagent Co. Ltd.

2.2 Methods

2.2.1 Synthesis

Hydrophobically modified inulin samples were synthesized by reaction between OSA and three inulin varieties (H25P, DS2 and XL) respectively. These modifications were carried out in aqueous solution under alkaline conditions, using the method as previously reported (Han *et al*., 2015).

2.2.2 Characterisation

NMR spectroscopy

^{1}H NMR spectra of the modified OSA-inulins were obtained using a 500 MHz NMR Spectrometer at 25 °C, according to the method as previously reported (Han *et al*., 2015). The sample (5 mg) was dissolved in 0.7 g of D_2O and transferred into a 5 mm thin wall sample NMR tube. The spectra were recorded at 25°C using the Pulse

Program ZG30 with a 30 degree pulse and a delay of 1s**,** together with Mnova 7.0 software.

Fourier-transform infrared spectroscopy (FTIR)

The OSA-inulin samples were dried in an oven at 70°C overnight. 1 mg of sample was milled with 100 mg of dried KBr using an agate mortar and pestle for several minutes to obtain a fine powder. A thin pellet was produced using a 15 ton manual press and a P/N 03000 13 mm pellet die (maximum load 10.0 tons) from Specac Limited. The FTIR spectra were recorded in the range 4000-400 cm^{-1} using a Perkin-Elmer FTIR spectrometer RX 1 taking 16 scans at a resolution of 4 cm^{-1}. Spectral analysis and display were performed using the interactive Read-IR3 version3.0 software (University of Sao Paulo, Brazil).

2.2.3 Solubilisation of beta-carotene

Stock solutions of 1% OSA-inulin were prepared and diluted to give various concentrations. 10 mg of beta-carotene was added to 10 mL of the solutions and left agitating at 40°C overnight. The solutions were then filtered to remove insoluble beta-carotene particles using Millex-GP 0.22 μm membrane filters (Millipore Ireland Ltd) before being transferred to disposable UV grade 10 mm path length cuvettes (CXA-110-0053 from Fisher Scientific Ltd). The absorbances were determined at the wavelength of 455 nm using a Lambda 25 UV/Vis Spectrometer (Perkin Elmer). The point at which the absorbance first increased corresponded to the critical aggregation concentration, CAC.

2.2.4 Size of the micellar aggregates

Dynamic light scattering

Dynamic light scattering (DLS) measurements were performed using the Zetasizer Nano ZS (Malvern Instruments Ltd, Malvern, UK) equipped with a 5 mW He-Ne laser (λ_0 = 632.8 nm) and a digital correlator at an angle of 175° to the incident beam, as described previously (Han *et al*., 2015). The temperature was controlled at 25±1˚C. The solutions, prepared as described above, were placed in disposable plastic cuvettes with a cross-sectional area of 1 cm^2. 15 runs were performed on each sample over collection times of 180 seconds. The hydrodynamic diameters were obtained from the Stokes-

Einstein relationship using the instrument software.

Transmission electron microscopy (TEM)

10 mg of beta-carotene was added to 10 mL of 0.07% (w/w) H25P; 0.06% DS2 (w/w) and 0.03% XL (w/w) respectively and the solutions were left agitating at 40°C overnight. The solutions were then filtered to remove insoluble beta-carotene particles using Millex-GP 0.22 μm membrane filters (Millipore Ireland Ltd) and one droplet of solution (with or without beta-carotene) was deposited onto a carbon-coated copper grid and excess sample was removed after 30 s with filter paper. The copper grids were slowly dried for 2 h at 25 ± 1 °C in a desiccator and later negatively stained by means of phosphotungstic acid (10 mg/mL) for 60 s. Observations were made with a JEM-2100F transmission electron microscope operating at 120 kV × 30 K (JEOL, Japan).

2.2.5 Encapsulation

Encapsulation of beta-carotene using OSA-inulin was facilitated by adding 0.5 g beta-carotene to a beaker containing 1L 0.1% OSA-inulin solutions (H25P, DS2 or XL, respectively) then stirring overnight in a water bath at 40 °C. The solutions were rotary evaporated to 40 mL and subsequently frozen in an ultra-low temperature freezer (SANYO, Japan) for 24 h (-70 °C). The samples were then freeze-dried using a FD-1C-50, Beijing, China freeze-dryer for 24 h (-48 °C, P = 9.8 Pa).

2.2.6 Release of beta-carotene in simulated stomach and small intestinal fluids

The encapsulated beta-carotene was passed through a simulated gastrointestinal digestion system as described by Zhang *et al*. (2016) with a little modification. 0.06 g encapsulated beta-carotene produced using H25P, DS2 and XL modified OSA-inulins respectively were dispersed in 30 mL buffer solutions (5 mM PBS, pH 7.0) in glass beakers and placed in a water bath at 37 °C with a shaker speed of 100 rpm for 15 min. The solutions were then mixed with 30 mL solution containing simulated gastric juice (0.0032 g/mL pepsin and adjusted to pH 2.5 using HCl). These mixtures were placed in a shaker at 100 rpm for 2 h at 37 °C to mimic stomach digestion. 2 mL portions of each of the dispersions were taken at various time intervals and filtered using Millex-GP 0.22

μm membrane filters into disposable UV-grade 10 mm path length cuvettes. The absorbances of the solutions were measured at 455 nm using a UV-visible spectrophotometer (TU-1900, Beijing).

Following this, 60 mL of each sample solution was placed in a 200 mL glass beaker located in a temperature-controlled (37°C) water bath, and the pH was adjusted to 7.0. Thereafter, 3 mL of simulated intestinal fluid (containing 10 mM $CaCl_2$ and 150 mM NaCl), followed by 7 mL of 46.9 mg/mL bile salt solution (produced by dissolving bile salt No.3 in 5 mM PBS, pH 7.0) were added, with constant stirring. The pH of the system was re-adjusted back to 7.0. The mixture was placed in a shaker at 100 rpm in a water bath at 37°C for 2 h. The UV-visible absorbances of these samples were measured as described above.

2.2.7 Dispersion of encapsulated beta-carotene at different pHs

0.06 g of encapsulated beta-carotene (in H25P, DS2 or XL, respectively) was dissolved in 30 mL buffer solution (5 mM PBS, pH 7.0) in a glass beaker. The pH values were adjusted to 3, 5, 7, 9 and 11 using either 0.1 M HCl or 0.1 M NaOH. The mixtures were then placed in a shaker at 100 rpm for 2 h at 25 °C in a temperature-controlled water bath. The UV-visible absorbances of these samples were measured in the manner described above.

2.2.8 Dynamic Vapor Sorption.

The moisture sorption behavior of the encapsulated beta-carotene particles was measured using a dynamic vapor sorption system (DVS-1, Surface Measurement Systems Ltd., London, U.K.) according to the method described in Hu *et al*. (2019). 5mg OSA-inulin encapsulated beta-carotene particles (H25P, DS2 or XL) was placed in the measurement chamber under a continuous N_2 gas flow at 25 °C. The relative humidity (RH) inside the chamber was step-changed from 0 to 90%, with 10% increments or decrements for sorption and desorption cycles, respectively. Equilibrated masses were recorded when the values of dm/dt were below 0.002% per minute.

3. Results and discussion

206 *3.1 Characterization*

207 The degrees of substitution of the OSA-inulins (H25P, DS2 and XL) were
208 determined by ^{1}H NMR and the spectra obtained are given in Supplementary data
209 Figure S1. The prominent peak at 4.70 ppm is from the solvent (Barclay *et al*., 2012).
210 The peaks between 3.30 and 4.23 ppm and the peak at 5.35 ppm are ascribed to the
211 inulin itself (Kulminskaya *et al*., 2003). By comparing the ^{1}H NMR spectra of our
212 modified samples with the spectrum for native inulin (in the same solvent D_2O)
213 obtained by Kulminskaya *et al*. (2003), it is evident from the additional peaks observed
214 that acetylation has occurred. The ^{1}H NMR signal at 0.8 ppm, being a triplet, shows
215 three protons of the terminal methyl group of the acyl chain, while the peaks at 1.26
216 ppm and 1.94 ppm correspond to the methyl and methylene groups of the
217 octenylsuccinic anhydride, which is consistent with previously reported data (Han *et*
218 *al*., 2015). Similar results were obtained for the OSA-inulins (H25P, DS2 and XL). The
219 extents of alkyl chain incorporation into the modified samples were calculated from the
220 ratios of peak areas at 0.8 ppm to the same ratios between 3.35-4.30 ppm and 5.35 ppm,
221 according the method previously described (Han *et al*., 2017). From the results
222 provided in Table 1, it can be seen that the OSA-inulins (H25P, DS2 and XL) with
223 different DPs have very similar degrees of substitution, DS. The DS is defined as:

224 $$\frac{\text{moles of OSA}}{\text{mole of fructose}} \times 100$$

226 Table 1. Degrees of substitution (DS) and critical aggregation concentrations (CAC) of
227 the hydrophobically modified OSA-Inulins.

Sample (OSA-inulin)	Degree of polymerization	Article cited	substitution / moles (%)	substituents per molecule	CAC (%) (Dye solubilisation)	CAC (%) (DLS)
H25P	2-8	(Evans *et al*., 2014)	19.2%	~1	0.07±0.005	0.007±0.005
DS2	2-18	(Han *et al*., 2017)	19.2%	~2	0.06±0.005	0.006±0.005
XL	20-23	(Ronkart, *et al*., 2007)	19.0%	~4	0.03±0.005	0.025±0.005

228

FTIR spectra of the unmodified inulin and modified OSA-inulin samples are presented in Supplementary data Figure S2. The peaks for the native inulin at 3398, 2930 and 1028 cm^{-1} indicate O-H stretching, CH_2 stretching and C-O-C bending, respectively (Fares, Salem, & Mai, 2011; Han *et al*., 2015; Kokubun *et al*., 2013). The spectra of OSA-inulins display two new peaks at 1576 and 1734 cm^{-1} due to the formation of the ester linkage. These peaks are assigned to asymmetric COO^- stretching and ester carbonyl stretching, respectively (Fares *et al*., 2011). The results are similar to our previous findings (Han *et al*., 2015). In studies on starch modification, it has previously been reported that the CH_2 stretching band at 2930 cm^{-1} increased after modification because of the contribution from the carbon chain associated with the alkenyl succinic group (Bai, Shi & Wetzal, 2009). However, as in our previous work, the CH_2 stretching band at 2930 cm^{-1} for the OSA-inulins with different DPs was not comparably enhanced (Han *et al*., 2015; Kokubun *et al*., 2013).

3.2 Critical aggregation concentration (CAC)

The UV-Vis absorbance values obtained for OSA-inulin solutions at different concentrations in the presence of beta-carotene are given in Figure 1. It is observed that the values increase significantly above a critical concentration which is attributed to the formation of micellar-like aggregates and the dissolution of the beta-carotene molecules in their hydrophobic cores. The CAC values for all the OSA-inulins are shown in Figure 1 and Table 1. They are, in general, similar to the value of 0.07% reported previously for OSA-modified inulin with a DS of ~29% (Han *et al*., 2015) and an order of magnitude lower than the values of 0.7-0.9% for OSA-modified inulin with DS 4-7% (Kokubun *et al*. 2013) which were determined using Sudan IV as the hydrophobic compound. The highest molar mass inulin XL sample was revealed to have formed micellar aggregates at a lower concentration than the other inulins (H25P and DS2) with lower molar masses. This may be due to the fact that each molecule of the modified XL inulin will contain a greater number of octenyl chains, with the distribution of the octenyl groups along the inulin chains also being a factor. The absorbance values for all three samples reached a plateau value of ~0.2 which was found to correspond to a

beta-carotene concentration of 10mg/L as determined from a previously constructed calibration curve for beta-carotene dissolved in cyclohexane Figure S3. The fact that a plateau absorbance value is attained is likely to be due to the limited solubility of beta carotene in the hydrophobic regions within the micellar aggregates. The solubility of beta carotene in water is 0.6mg/L and in hexane is 100mg/L. The loading capacity determined at the CAC for the three OSA inulin samples was calculated to be 12mg, 18mg and 25mg of beta carotene per g of H25P, DS2 and XL respectively. The increase in loading capacity with increasing molar mass is likely to be attributed to the fact that the number of alkenyl chains per inulin chains increases as the molar mass increases and the molecules may be able to associate through both intra- and inter-molecular interactions thus forming a more preferential hydrophobic region for the beta carotene to reside.

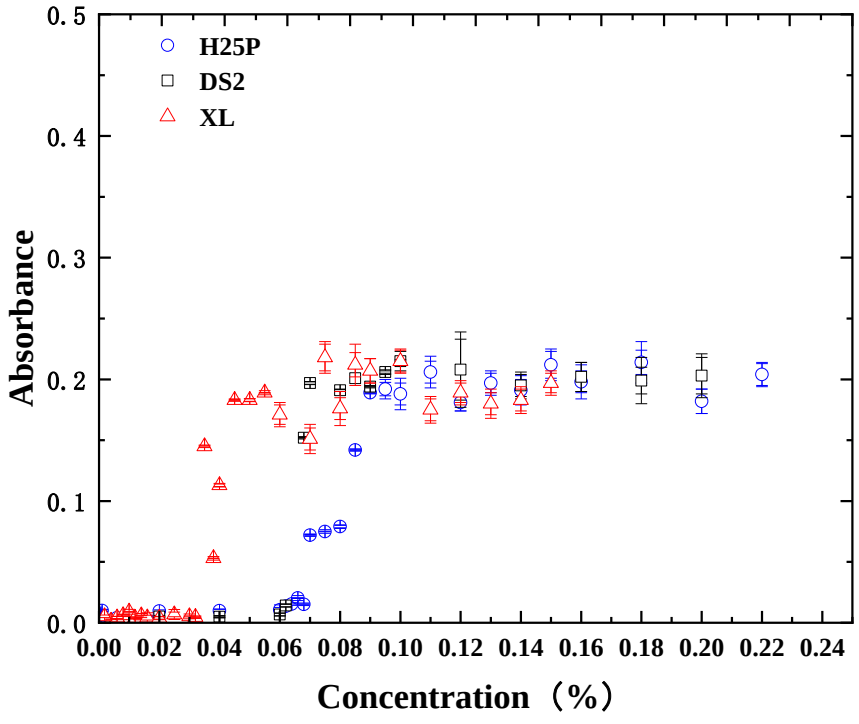

Figure 1. UV-Vis absorbance values at 455 nm of H25P, DS2, and XL inulin samples at varying concentrations, in the presence of beta-carotene.

The Z-average hydrodynamic diameters of the different OSA-inulins obtained by

DLS with and without beta-carotene encapsulated are shown as a function of concentration in Figure 2. In the absence of beta-carotene (Figure 2a) at low concentrations (below the CAC) the inulin molecules have a diameter of ~8-10 nm. The size does not appear to change for H25P but is seen to increase to ~12 nm for DS2 and XL, at concentrations corresponding to the respective CAC values reported above. The aggregates become slightly larger for samples with beta-carotene encapsulated (Figure 2b). The hydrodynamic sizes are similar to those reported previously (Kokubun et al., 2013).

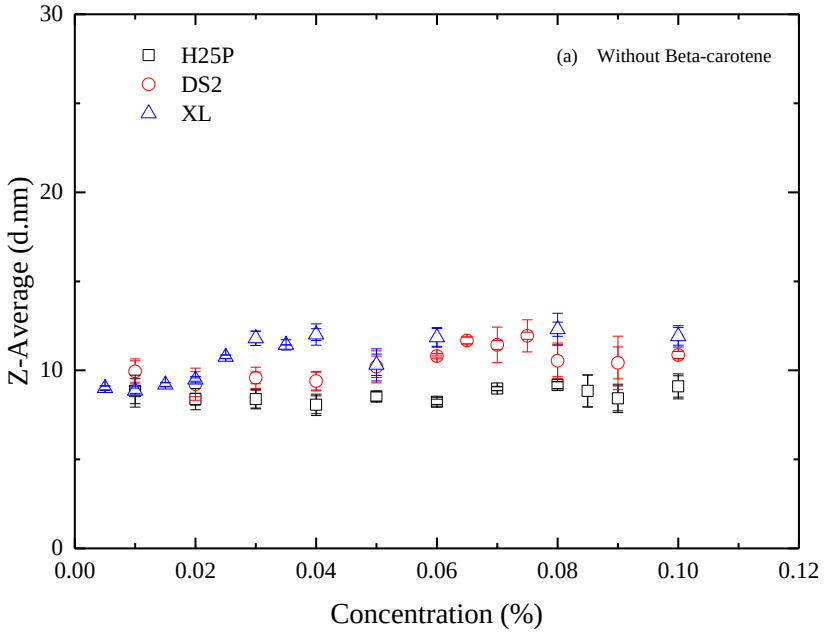

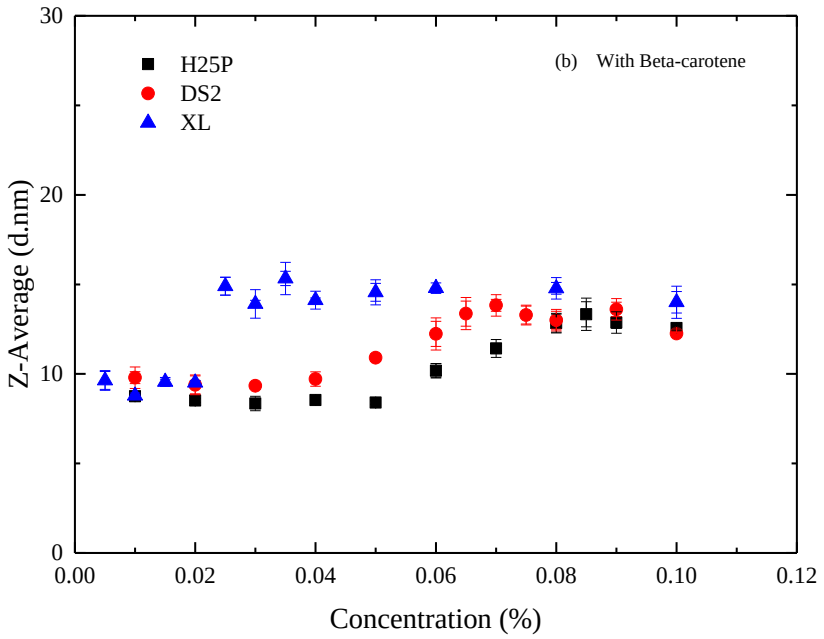

Figure 2. Z-average hydrodynamic diameter as a function of concentration for OSA-inulins (H25P, DS2 and XL) (a) without beta-carotene, (b) with beta-carotene.

The transmission electron micrographs of OSA-modified inulin with different DPs at their CAC (0.07% H25P, 0.06% DS2 and 0.03% XL) with and without encapsulated beta-carotene are shown in Figure 3. They indicate that the micellar aggregates are globular in shape. It is also noted that they are polydisperse with respect to size and that the size range is consistent with the values determined by DLS. The polydispersity is probably a reflection of two factors, namely that the inulin molecules for each sample will have a range of DS values and that the distribution along the polymer chain will vary significantly between molecules.

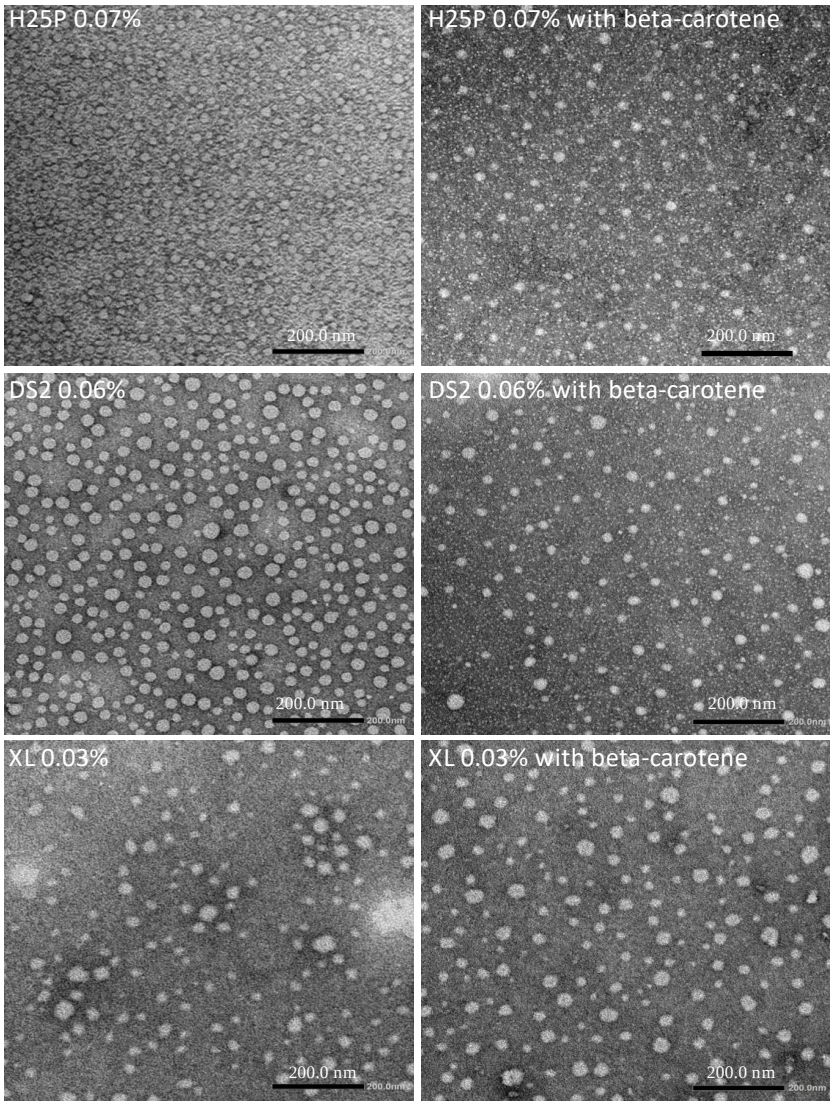

Figure 3. TEM micrographs of 0.07% H25P, 0.06% DS2 and 0.03% XL inulins with and without beta-carotene. Scale bar: 200 nm.

3.3 Encapsulation and release of beta-carotene

The release of encapsulated beta-carotene from freeze-dried OSA-inulin particulate samples was evaluated under simulated stomach (pH 2.5) and small intestine conditions (pH 7). The beta-carotene release was measured by passing the particles through the simulated gastrointestinal digestion system and the results are shown in Figure 4a. Photographs showing the release of beta-carotene in the simulated gastrointestinal digestion system at different times are provided in Figure 4b. The absorbances of the filtered solutions for all the OSA-inulins show no significant increase under simulated

stomach conditions, indicating there was no release of beta-carotene. The images of samples dispersed in the stomach phase after 120 minutes also confirm that the beta-carotene was not released at this stage. However, when the samples were subjected to simulated small intestine conditions, some difference was noticed. After 10 minutes, there was an increase of the absorbances for all the OSA-inulin particles, indicating the presence of dispersed micellar aggregates with beta-carotene dissolved within their hydrophobic cores. The reason why the beta-carotene encapsulated particles dissolve under the small intestinal conditions but not the simulated stomach conditions is attributed to the differences in pH. In the former scenario, the pH of the system is 7.0 and thus the carboxyl groups present in the head-group of the OSA molecules will be ionized and this will increase their solubility. In the latter case, the pH is 2.5 and the carboxyl groups will be predominantly non-ionized and hence the particles will have little tendency to dissolve.

The influence of pH on the dissolution of the particles is illustrated more clearly in Figure 5. At pH 3, only very small increases in absorbance were observed for all the OSA-inulins and was in the order H25P>DS2>XL which reflects their molar masses i.e. H25P<DS2<XL. With increasing pH, the absorbance values began to rise, indicating that micellar aggregates present had dissolved to a greater extent. In addition, the influence of the inulin molar masses became more significant. Furthermore, the lower molar mass H25P inulin dissolved much more readily at high pH, compared to the other inulin samples.

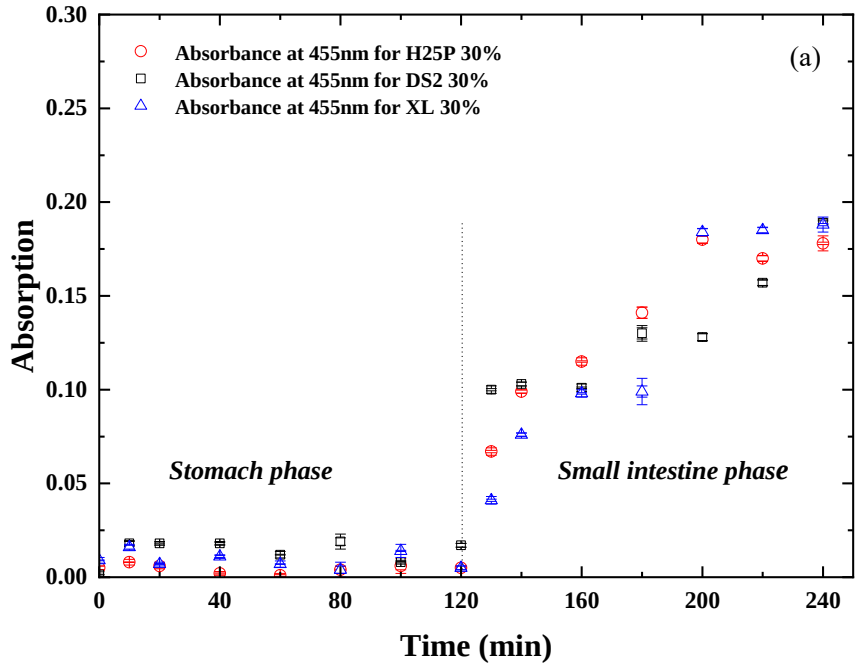

336

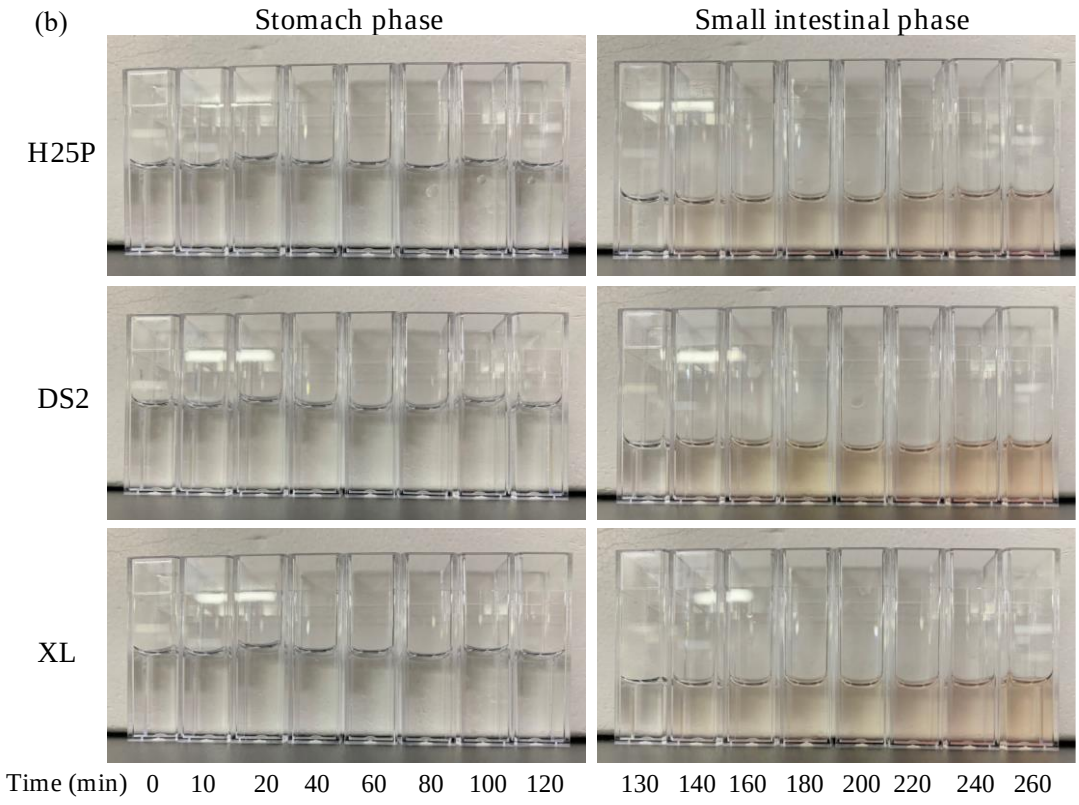

337

338 **Figure 4.** (a) Absorbances of OSA-inulin with different DPs (H25P, DS2 and XL) at
339 455 nm containing encapsulated beta-carotene as a function of time dispersed in the
340 simulated stomach and small intestine phases; (b) beta-carotene release in the simulated
341 stomach and small intestine phases at varying times.

342

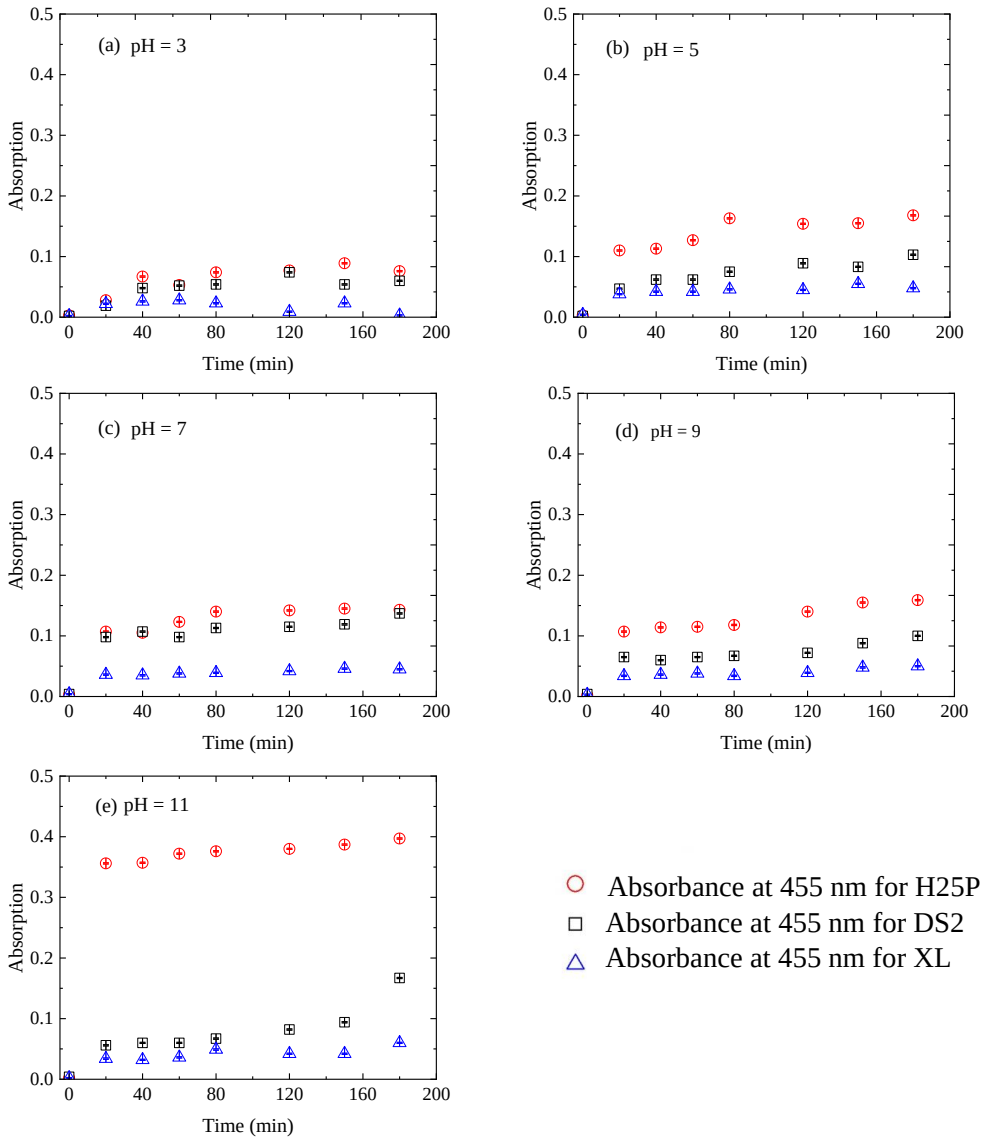

Figure 5. pH effect on absorbance of OSA-inulin with different DPs (H25P, DS2 and XL) encapsulated beta-carotene solid nanoparticles as a function of time.

3.4 Moisture resistance

The moisture sorption behaviors of the OSA-inulin particles with beta-carotene have been studied. The sorption isotherms of OSA-inulins with different DPs, obtained by conducting dynamic vapor sorption measurements, are shown in Figure 6. The particles were allowed to equilibrate at varying relative humidities (RHs) and the changes in equilibrium mass were recorded (as a function of RH) during sorption-

desorption cycles. According to the classification of Brunauer *et al*. (1940), moisture sorption isotherms of different OSA-inulin particles exhibit a sigmoidal (Type II) shape. Furthermore, the $a_w/w\ VS.\ a_w$ plots display a Type II-b shape, according to the Blahovec and Yanniotis (2009) classification. Desorption curves formed a hysteresis loop for all forms of OSA-inulin particles, as has been observed by several authors using different foodstuffs (Kachru & Matthes, 1976; Toğrul & Arslan, 2006). For H25P beta-carotene particles, the mass increased by around 19% when RH was elevated from 0 to 90%, while the corresponding values were approximately 17% for DS2 and XL particles with beta-carotene. The hysteresis loop areas for H25P, DS2 and XL was found to be in the order of H25P> DS2>XL, implying that the OSA-inulin, having a larger DP, possesses better moisture resistance.

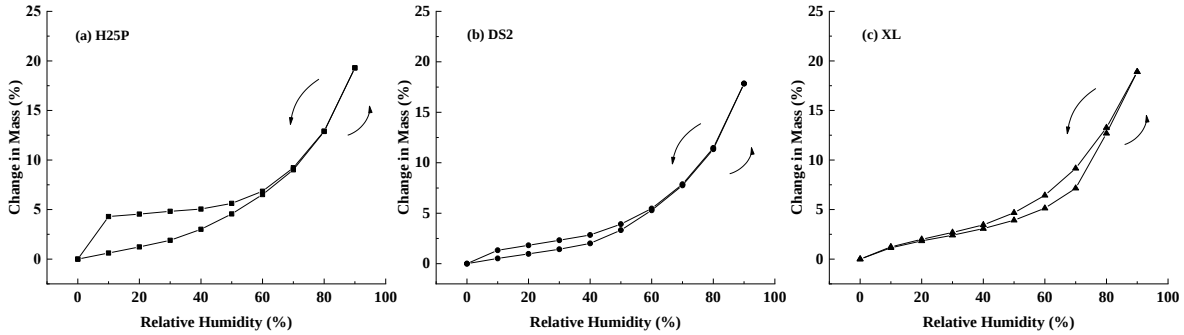

Figure 6. Sorption isotherms of freeze-dried OSA-inulin beta-carotene nanoparticles: (a) H25P (b) DS2 and (c) XL.

4. Conclusions

It has been shown that OSA-inulin samples with DS ~19 mol% will aggregate in aqueous solution, above a critical concentration, to form micellar aggregates. Moreover, it has been demonstrated that beta-carotene can readily dissolve in the hydrophobic cores of the micellar aggregates. On freeze-drying, the solutions produce OSA-inulin particles with encapsulated beta-carotene. It was found that the beta-carotene was not released when the particles were introduced into conditions experienced in the stomach but were released under conditions prevailing in the small intestine. It is evident that OSA-inulin can be used to dissolve water-insoluble hydrophobic compounds for

application in, for example, functional foods and pharmaceuticals. Since inulin is a type of dietary fiber and is not absorbed in the stomach, it also has medical applications in targeted drug delivery to the small and large intestine.

Acknowledgments

This work was supported by National Natural Science Foundation of China (No. 31701555).

References

Barclay, T., Ginic-Markovic, M., Johnston, M. R., Cooper, P. D., & Petrovsky, N. (2012). Analysis of the hydrolysis of inulin using real time 1 H NMR spectroscopy. *Carbohydrate Research,* 352(1), 117-125.

Bai, Y., Shi, Y., & Wetzel, D. L. (2009). Fourier transform infrared (FT-IR) microspectroscopic census of single starch granules for octenyl succinate ester modification. *Journal of Agricultural & Food Chemistry,* 57(14), 6443-6448.

Blahovec, J., & Yanniotis, S. (2009). Modified classification of sorption isotherms. *Journal of Food Engineering,* 91(1), 72-77.

Brunauer, S., Deming, L. S., Deming, W. E., & Teller, E. (1940). On A Theory of The Vander Waals Adsorption of Gases. *Journal of the American Chemical Society,* 62(7), 1723-1732.

Evans, M., Gallagher, J. A., Ratcliffe, I., & Williams, P. A. (2014). Functional properties of hydrophobically modified inulin in *Gums and Stabilisers for the Food Industry 17*, Proceedings of the Gums and Stabilisers for the Food Industry Conference, June 25−28, 2013, Glyndwr University, Wales, U.K. ; Williams, P.A., Philips, G.O., Eds.; Royal Society of Chemistry Special Publication No. 346; CPI Group: Croydon, U.K., 2014; pp 73−78.

Fares, M. M., Salem, M. T. S., & Mai, K. (2011). Inulin and poly(acrylic acid) grafted inulin for dissolution enhancement and preliminary controlled release of poorly water-soluble Irbesartan drug. *International Journal of Pharmaceutics,* 410(1), 206-211.

French, A. D. (1993). Recent Advances in the Structural Chemistry of Inulin. *Studies in Plant Science,* 3, 121-127.

Han, L., Ratcliffe, I., & Williams, P. A. (2015). Self-assembly and emulsification properties of hydrophobically modified inulin. *Journal of Agricultural and Food Chemistry,* 63(14), 3709-3715.

Han, L., Ratcliffe, I., & Williams, P. A. (2017). Synthesis, characterisation and physicochemical properties of hydrophobically modified inulin using long-chain fatty acyl chlorides. *Carbohydrate Polymers,* 178, 141-146.

Hu, B., Han, L., Ma, R., Phillips, G. O., Nishinari, K., & Fang, Y. (2019). All-Natural Food-Grade Hydrophilic-Hydrophobic Core-Shell Microparticles: Facile Fabrication Based on Gel-Network-Restricted Antisolvent Method. *ACS Appl Mater Interfaces,* 11(12), 11936-11946.

Kachru, R. P., & Matthes, R. K. (1976). The behaviour of rough rice in sorption. *Journal of Agricultural Engineering Research,* 21(4), 405-416.

Kokubun, S., Ratcliffe, I., & Williams, P. A. (2013). Synthesis, characterization and self-assembly of biosurfactants based on hydrophobically modified inulins. *Biomacromolecules,* 14(8), 2830-2836.

Kokubun, S., Ratcliffe, I., & Williams, P. A. (2015). The emulsification properties of octenyl- and dodecenyl- succinylated inulins. *Food Hydrocolloids,* 50, 145-149.

Kokubun, S., Ratcliffe, I., & Williams, P. A. (2018). The interfacial, emulsification and encapsulation properties of hydrophobically modified inulin. *Carbohydr Polym,* 194, 18-23.

Kulminskaya, A. A., Arand, M., Eneyskaya, E. V., Ivanen, D. R., Shabalin, K. A., Shishlyannikov, S. M., Saveliev, A. N., Korneeva, O. S., & Neustroev, K. N. (2003). Biochemical characterization of Aspergillus awamori exoinulinase: substrate binding characteristics and regioselectivity of hydrolysis. *Biochimica et Biophysica Acta (BBA) - Proteins and Proteomics,* 1650(1), 22-29.

Muley, P., Kumar, S., El Kourati, F., Kecharwani, S. S., & Tummala, H. (2016). Hydrophobically modified inulin as an amphiphilic carbohydrate polymer for

micellar delivery of paclitaxel for intravenous injection. *International Journal of Pharmaceutics*, 500, 32–41.

Ronkart, S. N., Deroanne, C., Paquot, M., Fougnies, C., Lambrechts, J.C., & Blecker, C. S. (2007). Characterization of the Physical State of Spray-Dried Inulin. *Food Biophysics,* 2(2-3), 83-92.

Srinarong, P., Hamalainen, S., Visser, M. R., Hinrichs, W. L. J., Ketolainen, J., & Frijlink, H. W. (2011). Surface active derivative of Inulin (Inutec SP1) is a superior carrieir for solid dispersions with a high drug load. *Journal of Pharmaceutical Sciences*, 100(6), 2333–2342.

Toğrul, H., & Arslan, N. (2006). Moisture Sorption Behaviour and Thermodynamic Characteristics of Rice stored in a Chamber under Controlled Humidity. *Biosystems Engineering,* 95(2), 181-195.

Zhang, Z., Zhang, R., Zou, L., Chen, L., Ahmed, Y., Al Bishri, W., & McClements, D. J. (2016). Encapsulation of curcumin in polysaccharide-based hydrogel beads: Impact of bead type on lipid digestion and curcumin bioaccessibility. *Food Hydrocolloids,* 58, 160-170.

List of Supplementary data Figures

Supplementary data Figure S1. Proton NMR spectra of OSA-inulins (H25P, DS2, and XL).

Supplementary data Figure S2. FT-IR spectra of unmodified inulin (Nature Inulin H25P) and OSA-Inulins (H25P, DS2, and XL).

Supplementary data Figure S3. UV absorbance of beta carotene dissolved in cyclohexane at 455nm as a function of concentration

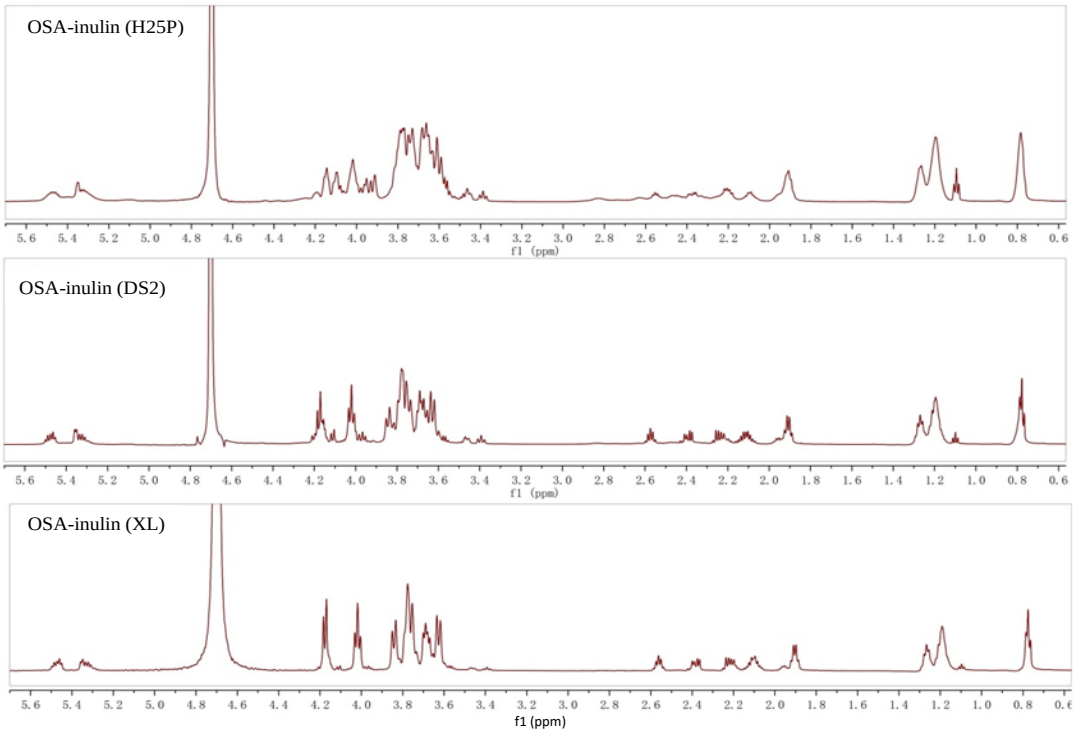

Supplementary data Figure S1. Proton NMR spectra of Hydrophobically Modified OSA-inulins (H25P, DS2, and XL).

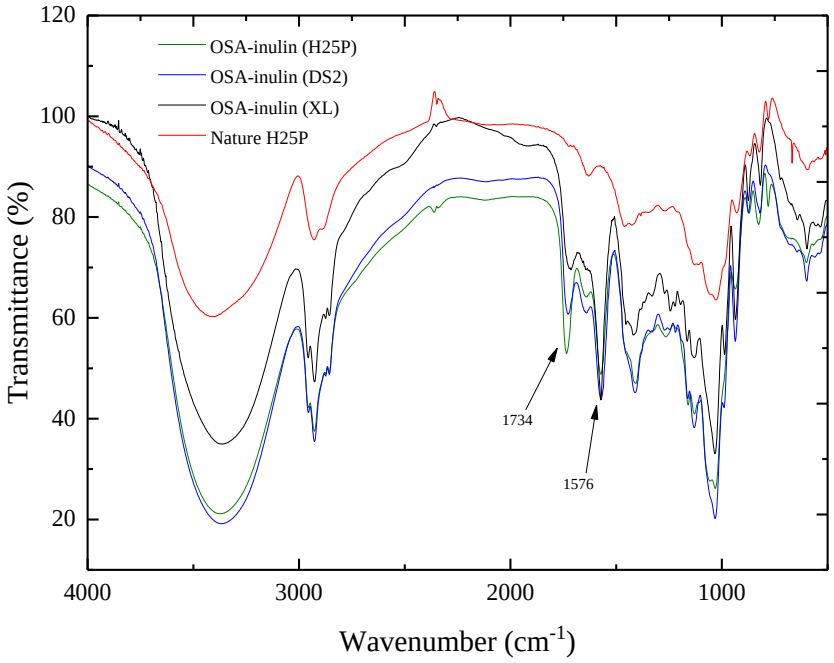

Supplementary data Figure S2. FT-IR spectra of unmodified inulin (Natural Inulin H25P) and Modified OSA-Inulins (H25P, DS2, and XL).

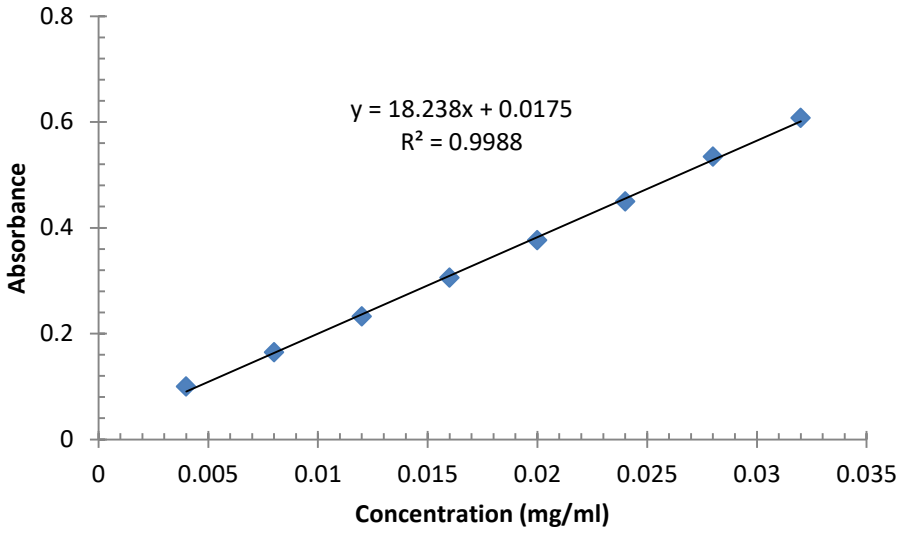

Supplementary data Figure S3. UV absorbance of beta carotene dissolved in cyclohexane at 455nm as a function of concentration